# The Characterisation of Molecular Boric Acid by Mass Spectrometry and Matrix Isolation Infrared Spectroscopy†

**J. Steven Ogden * and Nigel A. Young**
*Department of Chemistry, University of Southampton, Southampton SO9 5NH*

When crystalline orthoboric acid is heated *in vacuo* to *ca.* 40 °C, it vaporises to yield molecular $H_3BO_3$. The i.r. spectrum of this species isolated in low-temperature nitrogen matrices shows characteristic absorptions at 3 668.5 (*E'*), 1 426.2 (*E'*), 1 009.9 (*E'*), 675.0 (*A"*), 513.8 (*A"*), and 448.9 (*E'*) $cm^{-1}$ consistent with $C_{3h}$ symmetry. These spectral assignments are supported by extensive isotope labelling, and by a partial normal co-ordinate analysis.

Orthoboric acid ($H_3BO_3$) has been known as a crystalline solid for many years, and numerous papers have been devoted to its structure and reactivity.[1] However, experimental evidence for its existence as a vapour-phase *molecule* is remarkably sparse despite its frequent citing[2] as a classic example of a species possessing $C_{3h}$ symmetry. There is no reported structure determination for vapour-phase $H_3BO_3$, and at least one author[3] has stated that it does not exist. Nevertheless, its thermodynamic properties have been estimated,[4] and a number of studies have been carried out which point to its existence as a stable molecule.

Mass spectrometric studies[5] on the reaction between $H_2O$ and $B_2O_3$ at *ca.* 1 000 °C concluded that although the principal vapour species produced under these conditions is $HBO_2$, small amounts of $H_3BO_3$ may also be present. Margrave and co-workers[6] subsequently carried out a vapour-phase i.r. study of the $H_3BO_3$–$H_2O$ system over the temperature range 100—200 °C, and although few definite assignments could be obtained from the resulting spectra, they showed features consistent with the presence of molecular $H_3BO_3$. Transpiration experiments have also been carried out in this lower temperature range,[1] and several workers, notably Stackelberg,[7] Tazaki,[8] and Zachariasen[9] have drawn attention to the sublimation of boric acid, but did not identify the vapour species.

We have been studying the reactions between boric acid and alkali metal halides at elevated temperatures, using the combined techniques of matrix isolation and mass spectrometry. During the course of this work it became apparent that boric acid not only has a finite vapour pressure at *room temperature*, but that the vapour species contains boron, oxygen, and hydrogen. This paper describes our characterisation of this species, together with an interpretation of its i.r. spectrum.

## Experimental

Samples of boric acid with 'normal' isotope composition (*ca.* 80% $^{11}B$, *ca.* 20% $^{10}B$, *ca.* 100% $^{16}O$, and *ca.* 100% $^{1}H$) were obtained from Aldrich (gold label >99% pure) and used without further purification. This material was also used to prepare $^{18}O$- and $^{2}D$-enriched samples by dissolving the parent solid in isotopically labelled water ($H_2{}^{18}O$, 70 atom% or $D_2O$, 99 atom%) and allowing equilibration to take place over several days. At the end of this period, the solution was evaporated to dryness at room temperature. $^{10}B$-Enriched samples of boric acid were obtained by dissolving $B_2O_3$ (90 atom% $^{10}B$) in either $H_2{}^{16}O$, $H_2{}^{18}O$, or $D_2O$ and similarly evaporating to dryness.

† *Non-S.I. units employed:* eV = 1.60 × $10^{-19}$ J, bar = $10^5$ Pa, dyn = $10^{-5}$ N.

The general features of our matrix isolation equipment have been described elsewhere.[10] In the present study, samples of boric acid contained in Pyrex ampoules were initially pumped under high vacuum (< $10^{-6}$ mbar) at room temperature for 1—2 h in order to remove any absorbed water. Gentle warming to only 35—45 °C proved sufficient to generate a satisfactory flux of molecular species, and matrices were deposited by condensing this vapour at *ca.* 12 K with a large excess of nitrogen or argon (BOC 99.999%). Matrix i.r. spectra were subsequently obtained using Perkin-Elmer 983G and Bruker IFS 113V instruments. Under these deposition conditions, satisfactory spectra were obtained after typically 2—3 h, but the more intense absorptions could also be detected after *ca.* 5 h deposition without any external heating of the sample.

Mass spectrometric studies were carried out on the same samples, but somewhat higher temperatures (40—55 °C) were generally employed in order to discriminate against hydrocarbon background signals. A VG SXP400 quadrupole spectrometer interfaced with a microcomputer was employed for routine studies and spectra were also run using the solids probe on an AEI MS-30 instrument which is capable of much higher sensitivity.

The sampling arrangements for our quadrupole mass spectrometric and matrix studies are identical, and samples of known isotope composition could therefore be transferred directly between the two rigs with minimal risk of contamination.

## Results and Discussion

*Mass Spectrometric Studies.*—Figure 1(*a*) shows part of a typical 20 eV mass spectrum obtained by heating 'normal' boric acid to *ca.* 40 °C. The prominent ions in this spectrum at *m/e* 44/45 and 61/62 may readily be identified as $[B(OH)_2]^+$ and $[B(OH)_3]^+$, and the only other boron-containing species detected in these studies was a minute amount (<0.5%) of $[H_3B_3O_6]^+$. The appearance potentials for $[B(OH)_2]^+$ and $[B(OH)_3]^+$ were estimated as 13.8 ± 0.5 and 10.8 ± 0.5 V respectively, and indicate a typical daughter–parent relationship. Figure 1(*b*) shows the mass spectrum obtained under similar conditions from a sample of $^{10}B$- and $^{18}O$-enriched boric acid. In addition to establishing the presence of boron and oxygen in these ions, the main reasons for obtaining such spectra were first to establish whether isotope scrambling was complete, and secondly to calculate the extent of $^{18}O$ enrichment. Thus the spectrum in Figure 1(*b*) corresponds closely to an isotopically scrambled sample containing *ca.* 90 atom% $^{10}B$ and *ca.* 60 atom% $^{18}O$. Similar studies were also carried out on deuteriated boric acid. As might be expected, $H_3B^{16}O_3/D_2O$ exchange was found to be very rapid, but $H_3B^{16}O_3/H_2{}^{18}O$

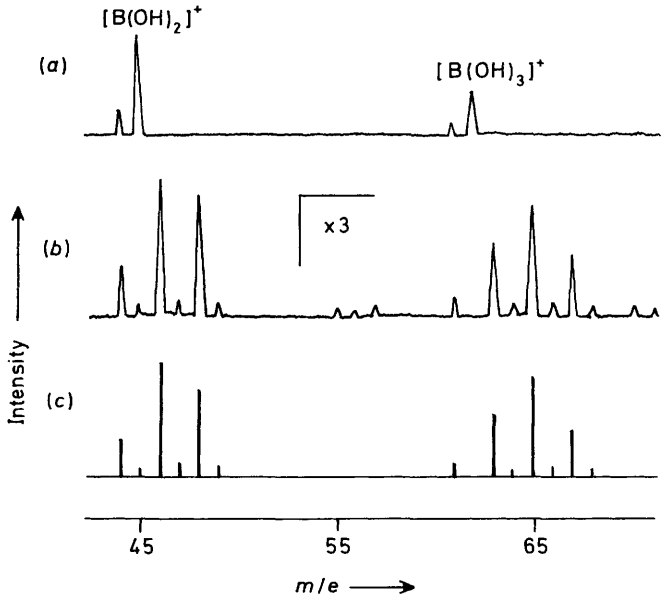


**Figure 1.** Mass spectra (20 eV) obtained from samples of boric acid at 40 °C. (*a*) Sample with normal isotopic composition; (*b*) sample enriched with $^{10}B$ and $^{18}O$, and (*c*) calculated spectra for $[B(OH)_2]^+$ and $[B(OH)_3]^+$ assuming 90% $^{10}B$ and 60% $^{18}O$ with 100% $^{1}H$

scrambling was a significantly slower process requiring several days to ensure completion.

*Matrix Isolation Studies.—Preliminary results.* Figure 2(*a*) shows a typical i.r. survey spectrum obtained after cocondensing 'normal' boric acid vapour generated at *ca.* 35 °C with a large excess of nitrogen at *ca.* 12 K. Prominent peaks are observed at *ca.* 3 726, 3 668.5, *ca.* 1 597, 1 478.0, 1 426.2, 1 009.9, 675.0, and 513.8 $cm^{-1}$, with weaker features at *ca.* 3 633, *ca.* 1 460, *ca.* 1 080, 700.9, and 448.9 $cm^{-1}$. Three of these absorptions (denoted *) may be identified as arising from $H_2O$, but the remaining features have not been previously observed. Figure 2(*b*) shows the nitrogen matrix spectrum obtained under identical conditions from a sample of $^{10}B$-enriched boric acid. All the features present in Figure 2(*a*) may also be observed in this spectrum, but the relative intensities of certain pairs of bands have altered significantly. In particular, the features at 1 478.0 and 1 426.2 $cm^{-1}$ which appear in Figure 2(*a*) with an approximate intensity ratio of 1 : 2 are seen in Figure 2(*b*) with a corresponding ratio of *ca.* 10:1, and similar intensity changes are evident in the doublet at 700.9/675.0 $cm^{-1}$. This effect is a direct result of changing the $^{10}B:^{11}B$ isotope abundance, and highlights those modes which involve significant boron atom motion. The weak peaks at *ca.* 1 460 and *ca.* 1 080 $cm^{-1}$ remained broad under higher resolution, and did not appear to correlate with any of the more intense features.

Several experiments were also carried out in argon matrices, and although a very similar pattern of new bands was produced, the absorptions were significantly broader than in nitrogen. On the basis of the mass spectrometric results, the i.r. bands observed in these preliminary experiments are provisionally assigned to *molecular* boric acid, and Table 1 summarises the nitrogen matrix frequencies attributed to $H_3{}^{11}BO_3$. Subsequent experiments involving $^{18}O$ or $^{2}D$ enrichment were all carried out in nitrogen matrices. These isotope experiments yielded a large number of bands, and a selection of these is included in Tables 2 and 3.

*I.r. spectral assignments.* The assignments proposed for the various matrix frequencies listed in Table 1 are based on a group frequency approach, and at this level of description may be

**Table 1.** I.r. active vibrational fundamentals ($cm^{-1}$) for $H_3{}^{11}BO_3$ in different phases

| Solid[a] | Vapour[b] | Nitrogen matrix[c] | Assignment |
|---|---|---|---|
| 3 150 | 3 750(?) | 3 668.5 | *E'* OH stretch |
| 1 428 | 1 430 | 1 426.2 | *E'* BO stretch |
| 1 183 | 1 015(?) | 1 009.9 | *E'* HOB bend |
| 648 | — | 675.0 | *A''* $BO_3$ bend |
| 544 | — | 448.9 | *E'* $BO_2$ bend |
| 824 | 303(?) | 513.8 | *A''* torsion |

[a] Refs. 1 and 11. [b] Refs. 6 and 16. [c] This work: frequency accuracy ±0.7 $cm^{-1}$.

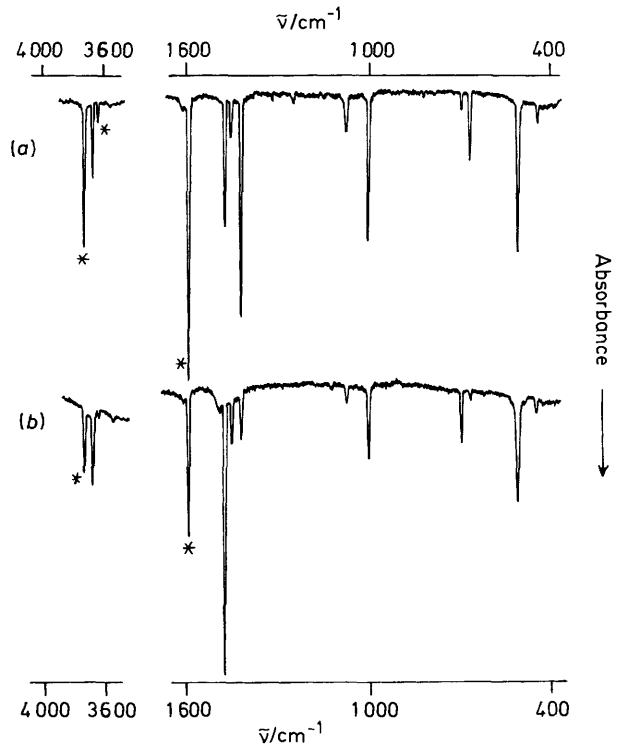


**Figure 2.** Low-resolution i.r. spectra obtained from boric acid isolated in nitrogen matrices at *ca.* 12 K. (*a*) Spectrum obtained from normal boric acid and (*b*) spectrum obtained from sample enriched with 90% $^{10}B$. The bands denoted (*) are due to monomeric $H_2O$

compared with previous data for crystalline boric acid.[1,11] This material has a structure[9,12,13] which consists of a network of $B(OH)_3$ units linked by hydrogen bonding. As a result, one might anticipate substantial differences in frequency and intensity between the isolated molecule and the solid as regards *hydrogen* atom motion, but might hope for a closer correspondence when considering the vibrations of the $BO_3$ unit.

Unfortunately, there is considerable variation in the literature[1] concerning the frequencies and assignments for '$H_3BO_3$' in the solid. However the combined results of Bethell and Sheppard,[14] and Servoss and Clark[15] have gained general acceptance,[11] and for the purposes of comparison, Table 1 summarises their i.r. fundamentals in the solid. Also included in this Table are the gas-phase data reported by Margrave.[6,16]

Comparison of the matrix, gas-phase, and solid data supports the expectation that frequencies assigned to $BO_3$ motion show a very satisfactory correspondence, whilst significant differences occur in modes involving hydrogen atom motion, notably in the O–H stretching region, and in the assignment of the torsion modes. In attempting to understand the spectrum of *molecular*

**Table 2.** Observed and calculated frequencies ($cm^{-1}$) for selected fundamentals of isotopically labelled boric acid

(*i*) Out-of-plane $BO_3$ bend

| Observed | Calculated[a] | Assignment |
|---|---|---|
| 675.0 | 674.4 | $^{11}B^{16}O_3$ |
| 672.6 | 672.1 | $^{11}B^{16}O_2{}^{18}O$ |
| 670.2 | 669.7 | $^{11}B^{16}O^{18}O_2$ |
| 668.1 | 667.4 | $^{11}B^{18}O_3$ |
| 700.9 | 701.3 | $^{10}B^{16}O_3$ |
| 698.6 | 699.0 | $^{10}B^{16}O_2{}^{18}O$ |
| 696.4 | 696.8 | $^{10}B^{16}O^{18}O_2$ |
| 694.1 | 694.5 | $^{10}B^{18}O_3$ |

(*ii*) Torsion modes

| Observed | Calculated[b] | Assignment |
|---|---|---|
| — | 577.7 | $E''$ $H_3BO_3$ |
| 513.8 | 513.8 | $A''$ $H_3BO_3$ |
| 408.4 | 408.3 | $A''$ $H_2DBO_3$ |
| 541.8 | 541.7 | |
| — | 577.7 | |
| 561.2 | 561.4 | $A''$ $HD_2BO_3$ |
| 390.5 | 390.3 | |
| — | 434.3 | |
| 376.0 | 375.7 | $A''$ $D_3BO_3$ |
| — | 434.3 | $E''$ $D_3BO_3$ |

(*iii*) OH stretching modes

| Observed | Calc. A[c] | Calc. B[d] | Assignment |
|---|---|---|---|
| — | 3 672.6 | 3 672.6 | $A'$ $H_3B^{16}O_3$ |
| 3 668.5 | 3 668.5 | 3 668.5 | $E'$ $H_3B^{16}O_3$ |
| | 3 668.5 | 3 668.5 | $A'$ $H_3B^{16}O_2{}^{18}O$ |
| 3 658.2 | 3 657.6 | 3 658.1 | |
| 3 671.8 | 3 671.5 | 3 671.5 | |
| 3 670.2 | 3 670.2 | 3 670.2 | $A'$ $H_3B^{16}O^{18}O_2$ |
| 3 659.2 | 3 658.9 | 3 659.4 | |
| | 3 656.5 | 3 657.1 | |
| 3 657.6 | 3 656.5 | 3 657.1 | $E'$ $H_3B^{18}O_3$ |
| — | 3 660.6 | 3 661.2 | $A'$ $H_3B^{18}O_3$ |
| — | 3 672.6 | 3 672.6 | $A'$ $H_3BO_3$ |
| 3 668.5 | 3 668.5 | 3 668.5 | $E'$ $H_3BO_3$ |
| | 3 668.5 | 3 668.5 | $A'$ $H_2DBO_3$ |
| 3 671.1 | 3 671.2 | 3 671.2 | |
| 2 705.8 | 2 670.2 | 2 705.9 | |
| 3 669.7 | 3 669.9 | 3 669.9 | $A'$ $HD_2BO_3$ |
| 2 707.7 | 2 671.2 | 2 706.9 | |
| | 2 669.2 | 2 704.9 | |
| 2 704.6 | 2 669.2 | 2 704.9 | $E'$ $D_3BO_3$ |
| — | 2 672.4 | 2 707.7 | $A'$ $D_3BO_3$ |

[a] Assuming force constant $K = 0.2665$ mdyn $Å^{-1}$. [b] Assuming $F_\tau = 0.0644$, $F_{\tau\tau} = -0.0035$ mdyn $Å^{-1}$ and $\beta = 131°$. [c] Assuming harmonic motion, with $F_d = 7.468$ and $F_{dd} = 0.0056$ mdyn $Å^{-1}$. [d] Assuming $\omega_e x_e = 90$ $cm^{-1}$, with $F_d = 8.219$ and $F_{dd} = 0.0064$ mdyn $Å^{-1}$.

boric acid, we therefore decided to base our analysis entirely on matrix data, and to rely on the isotope patterns generated by $^{18}O$ and $^{2}D$ enrichment for both qualitative and quantitative support. Before discussing these results in detail, however, it is helpful to consider the i.r. spectrum predicted for molecular $H_3BO_3$.

There are relatively few *molecular* species with the stoicheiometry $X(YZ)_3$, and the generally accepted shape for $H_3BO_3$ ($C_{3h}$) is based entirely on the solid phase. Nevertheless, this must also be considered the most likely vapour-phase structure by comparison with $B(OMe)_3$ which is known to have[17] a $C_{3h}$ framework. However, departures from the $C_{3h}$ structure to symmetry $C_3$ or lower by loss of overall planarity are possible, and it is not inconceivable that a $D_{3h}$ structure with either linear

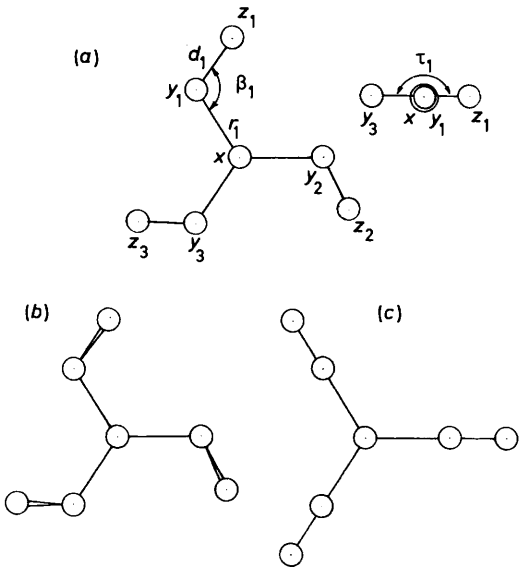


**Figure 3.** Possible structures for molecular boric acid. (*a*) $C_{3h}$ model for general $X(YZ)_3$ species, with definitions of internal co-ordinates, (*b*) $C_3$ model, and (*c*) $D_{3h}$ model

BOH groups, or symmetrically placed bridging protons might be preferred. Various possible structures are shown in Figure 3.

The approach we have adopted, however, is to assign the boric acid spectra initially on the basis of $C_{3h}$ symmetry, and then to consider whether there are any features which might indicate a departure from this model.

*Vibrational Analysis.—Results of isotope substitution.* Despite the lack of experimental data, the vibrational analysis of the $C_{3h}$ $X(YZ)_3$ framework has attracted considerable attention.[3,11,18] Using standard methods it may be readily shown that $\Gamma_{vib.} = 3A' + 2A'' + 4E' + E''$ and that the i.r. active modes are $2A'' + 4E'$. A general description of the various modes using internal co-ordinates then leads to the following six i.r. spectral features: $\nu$(OH), $E'$; $\nu$(BO), $E'$; $\delta(BO_2)$, $E'$; $\delta$(HOB), $E'$; $\gamma(BO_3)$, $A''$; and $\tau$(HOBO), $A''$. The notation adopted here follows the convention used by Cyvin *et al.*[18] These descriptions also serve as indications of the likely effect of isotope substitution. Thus all modes nominally involving H-atom motion should show a large (*ca.* 30%) frequency shift on deuteriation. In addition, *partial* $^{2}D$ or $^{18}O$ enrichment would be expected to permit a distinction between degenerate and non-degenerate modes *via* characteristic isotope patterns. Distortions from $C_{3h}$ symmetry should also be detectable from such patterns in addition to the spectral changes arising from different selection rules for the parent species.

Our initial isotope studies on boric acid (some of which are displayed in Figure 2) showed that the nitrogen matrix spectra were sufficiently well resolved to reveal isotope effects on all the observed frequencies. A large number of experiments were carried out on doubly- and triply-labelled boric acid and the results of these, together with their interpretation are most conveniently discussed in the context of the five i.r. spectral regions associated with the various $H_3BO_3$ absorptions.

*Spectral region* 650—750 $cm^{-1}$. The nitrogen matrix i.r. spectrum of 'normal' boric acid (20% $^{10}B$, 80% $^{11}B$) in this region shows sharp features at 700.9 and 675.0 $cm^{-1}$, with an intensity ratio *ca.* 1:4, and a typical spectrum is shown in Figure 4(*a*). An almost identical spectrum is obtained for all levels of deuterium enrichment, with the above frequencies affected by less than *ca.* 1 $cm^{-1}$. This spectral region is too low for O–H or B–O stretching modes and absorptions here must arise from

**Table 3.** Spectral features ($cm^{-1}$) arising from the ν(BO), δ($BO_2$), and δ(HOB) $E'$ modes as a result of $^{18}O$ or $^{2}D$ enrichment

| Mode | $^{18}O$ Enrichment | | | $^{2}D$ Enrichment | | |
|---|---|---|---|---|---|---|
| ν(BO) | $^{10}B$ | $^{11}B$ | Species | $^{10}B$ | $^{11}B$ | Species |
| | 1 478.0 | 1 426.2 | 16–16–16 | 1 478.0 | 1 426.2 | 1–1–1 |
| | 1 475.7 | 1 424.5 | 16–16–18 | 1 476.8 | 1 421.6 | 1–1–2 |
| | 1 469.0 | 1 417.5 | | 1 457.5 | 1 410.7 | |
| | 1 471.0 | 1 419.0 | 16–18–18 | 1 468.3 | 1 417.7 | 1–2–2 |
| | 1 463.0 | 1 411.9 | | 1 455.6 | (1 403.2) | |
| | 1 461.2 | 1 409.7 | 18–18–18 | 1 452.7 | | 2–2–2 |
| δ($BO_2$) | $^{10}B$ | $^{11}B$ | Species | $^{10}B$ | $^{11}B$ | Species |
| | 450.5 | 448.9 | 16–16–16 | 450.5 | 448.9 | 1–1–1 |
| | 445.8 | 444.5 | 16–16–18 | 449.2 | 447.8 | |
| | 442.9 | 441.2 | | 436.9 | 436.6 | 1–1–2 and |
| | 440.0 | 438.6 | 16–18–18 | 432.6 | 431.0 | 1–2–2 |
| | 436.4 | 434.8 | | 420.7 | 419.3 | |
| | 431.9 | 430.7 | 18–18–18 | 405.2 | 404.7 | 2–2–2 |
| δ(HOB) | $^{10}B/^{11}B$ | | Species | $^{10}B/^{11}B$ | | Species |
| | 1 009.9 | | 16–16–16 | 1 009.9 | | 1–1–1 |
| | 1 007.6 | | 16–16–18 | 1 011.4 | | 1–1–2 |
| | 1 002.3 | | and | 887.5 | | |
| | 996.6 | | 16–18–18 | 1 014.9 | | 1–2–2 |
| | 999.5 | | 18–18–18 | 894.5 | | |
| | | | | 825.5 | | 2–2–2 |
| | | | | (831.5) | | |

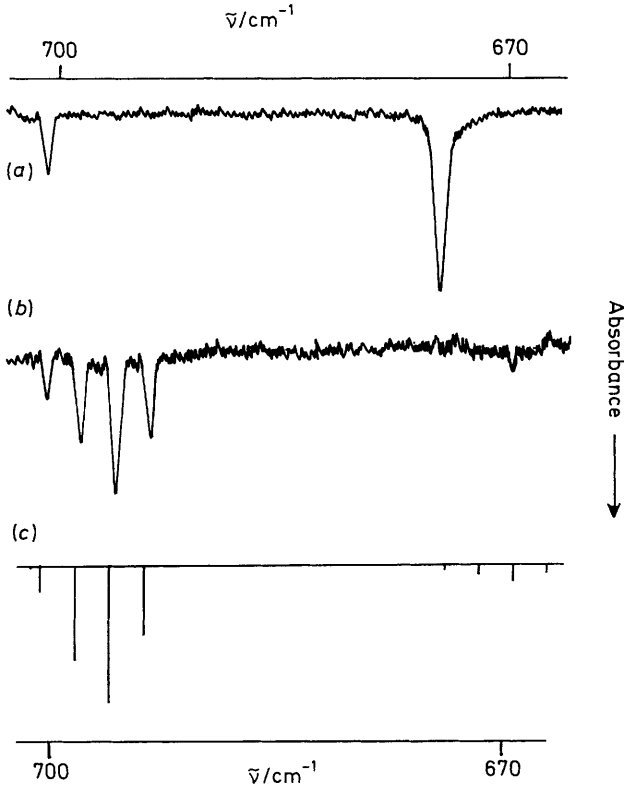


**Figure 4.** Isotope patterns associated with the $A''$ $BO_3$ bend. (*a*) Spectrum obtained from normal boric acid, (*b*) spectrum obtained from sample enriched with 90% $^{10}B$ and 60% $^{18}O$, and (*c*) spectrum calculated for sample containing 90% $^{10}B$ and 60% $^{18}O$

torsion modes or more conventional bending modes. The boron isotope effect is quite large, and the negligible effect with deuteriation indicates that, for $C_{3h}$ symmetry, this mode corresponds to either the in-plane ($E'$) or out-of-plane ($A''$) bending mode of the $BO_3$ unit.

Figure 4(*b*) shows the spectrum obtained from a sample of boric acid containing *ca.* 90% $^{10}B$ and *ca.* 60% $^{18}O$ (with 100% $^{1}H$). A prominent quartet is observed in the region of the band at 700.9 $cm^{-1}$ and similar experiments with higher levels of $^{11}B$ enrichment reveal a corresponding quartet pattern on the absorption at 675.0 $cm^{-1}$. These additional features arise from $H_3B^{16}O_2{}^{18}O$, $H_3B^{16}O^{18}O_2$, and $H_3B^{18}O_3$, and the frequencies of all the bands observed in this region, together with their assignments, are listed in Table 2. The individual components of these quartets show an intensity variation which corresponds to the binomial distribution expected for *three* equivalent oxygen atoms participating in a *non*-degenerate vibration. These features must therefore be associated with the $A''$ $BO_3$ mode.

Finally, Figure 4(*c*) shows the result of a spectral simulation in this region for the isotope mixture in Figure 4(*b*). Although knowledge of the position of the second $A''$ (torsion) mode in the $H_3BO_3$ would be required to calculate such an isotope pattern exactly, the fact that there is little or no deuterium isotope effect on this mode indicates that the two $A''$ modes are effectively decoupled. The spectrum in Figure 4(*c*) has therefore been calculated by considering the $BO_3$ unit in isolation, and using the appropriate secular equation (see Appendix) and known isotope abundances. The agreement is very satisfactory, and the numerical data from this analysis are included in Table 2.

*Spectral regions* 3 600—3 700 $cm^{-1}$ *and* 2 650—2 750 $cm^{-1}$. These are the spectral regions associated with O–H and O–D stretching respectively in *non*-hydrogen-bonded systems, and Figure 5(*a*) shows a typical nitrogen matrix spectrum obtained from 'normal' $H_3BO_3$. The bands at *ca.* 3 726 and *ca.* 3 633 $cm^{-1}$ are due to matrix isolated $H_2O$ monomer,[19] but the central feature at 3 668.5 $cm^{-1}$ is assigned to $H_3BO_3$. This band is shown under higher resolution in Figure 5(*b*), and proved to be insensitive to changes in the $^{10}B:^{11}B$ ratio. Enrichment with $^{18}O$ however [Figure 5(*c*)] produced two shoulders at 3 671.8 and 3 670.2 $cm^{-1}$ on the high-frequency side of the band at 3 668.5 $cm^{-1}$, and another relatively intense, asymmetric,

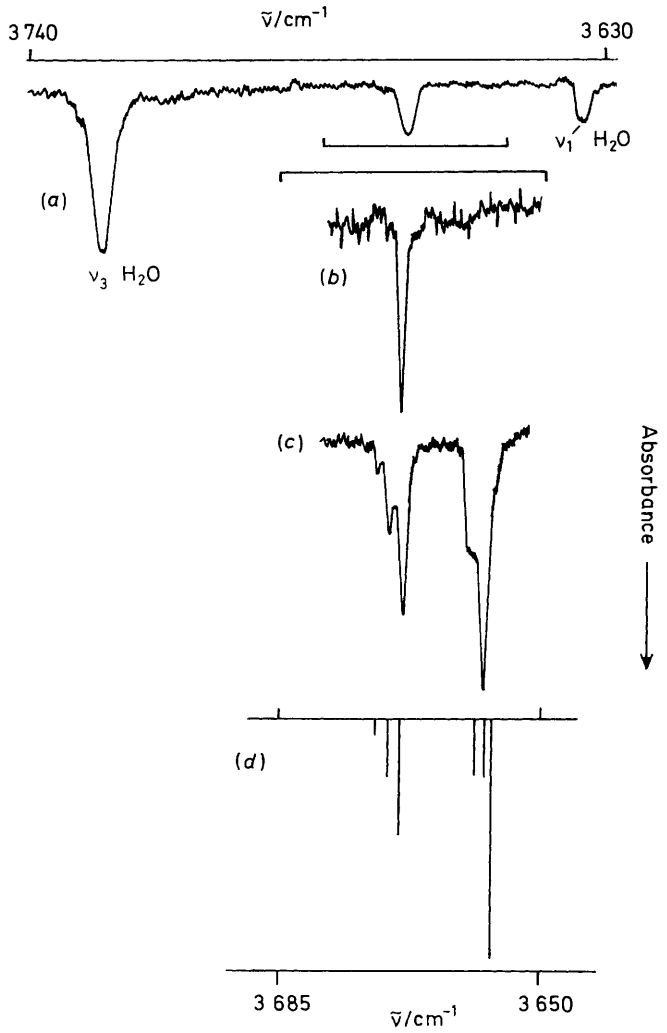


**Figure 5.** Isotope patterns associated with the OH stretching region. (*a*) Spectrum obtained from normal boric acid, (*b*) as (*a*), but with higher resolution, (*c*) spectrum obtained from sample of $^{18}O$-enriched boric acid, and (*d*) spectrum calculated for 60% $^{18}O$ enrichment (and assuming harmonic vibrations)

absorption at *ca.* 3 658 $cm^{-1}$. In contrast to the $^{18}O$ isotope structure on the *A*″ $BO_3$ mode, this pattern is highly asymmetric, and the intensities bear little resemblance to binomial statistics. Such a pattern is, however, characteristic of partial isotope substitution in a doubly-degenerate mode involving three weakly coupled oscillators.

This type of pattern was first encountered in connection with the analysis of the terminal CO stretching modes in $D_{3h}$ transition metal tricarbonyls,[20] and shortly afterwards was observed experimentally in $Pd(N_2)_3$.[21] In these earlier studies, the high-frequency separation approximation was assumed, and the only coupling between the CO or $N_2$ groups was through off-diagonal *F*-matrix terms. In $B(OH)_3$ an analogous situation arises regarding the OH stretching modes, and even though the symmetry here is taken to be $C_{3h}$, it turns out that the secular equations are identical to those derived for $D_{3h}$. As a result, it should be possible to simulate the observed isotope pattern using a simple two-parameter force field. The appropriate *G* and *F* matrix elements are given in the Appendix. The results of this analysis are displayed in Table 2 and Figure 5(*d*), and the agreement is quite satisfactory. In addition to providing further confirmation of the presence of a three-fold axis in $H_3BO_3$, this analysis predicts a value of 3 672.6 $cm^{-1}$ for the totally symmetric $^{16}OH$ stretch. This mode is i.r. *inactive* for $C_{3h}$ symmetry, but if boric acid were to possess a lower symmetry such as $C_3$ in which the OH groups are no longer co-planar [*e.g.* Figure 3(*b*)] it should be observable in the spectrum.

The effect on the O–H modes of deuterium enrichment is predictably very large, and corresponding O–D stretching modes are observed at *ca.* 2 700 $cm^{-1}$. In particular, we assign the *E*′ mode in $D_3B^{16}O_3$ at 2 704.6 $cm^{-1}$, but partial deuteriation also generates new absorptions at 3 669.7 and 3 671.1 $cm^{-1}$ which may be assigned to OH modes in $HD_2BO_3$ and $H_2DBO_3$ respectively. These new bands are included in Table 2.

In principle, it should be possible to simulate the H/D isotope patterns using the same two force constants as for the $^{16}O/^{18}O$ analysis above, but the results of this calculation are disappointing in that all the calculated O–D frequencies are *ca.* 30 $cm^{-1}$ too low. This discrepancy could be due to a breakdown of the high-frequency separation approximation, but it might also be due to anharmonicity, and in this event, one might obtain much better agreement by employing some form of anharmonic correction.

For the diatomic species $^{16}OH$ the $\omega_e$ and $\omega_e x_e$ values are 3 735.2 and 82.81 $cm^{-1}$ respectively,[22] and the approach adopted was initially to apply this same correction to the observed *E*′ mode in $H_3B^{16}O_3$ to produce a harmonic frequency $\omega_{E'}$ = 3 834.1 $cm^{-1}$. This value was then used to calculate sets of principal and interaction force constants which in turn generated the harmonic frequencies of all the isotope species. These ω values were then converted back to transition frequencies using standard procedures,[22] and the results compared with experiment. Frequency agreement over the entire O–H to O–D range was now possible to better than *ca.* 1 $cm^{-1}$ and even closer agreement was obtained by taking an initial value of 90 $cm^{-1}$ for $\omega_e x_e$. The results of this calculation are also included in Table 2.

*Spectral region* 1 400—1 500 $cm^{-1}$. Figure 6(*a*) shows a typical nitrogen matrix spectrum in this region obtained from a sample of 'normal' boric acid. Two sharp bands are observed at 1 478.0 and 1 426.2 $cm^{-1}$ with an intensity ratio of 1:4 and are identified as the $^{10}B$ and $^{11}B$ components of the *E*′ $BO_3$ stretch (Table 1). The weak broad feature at *ca.* 1 460 $cm^{-1}$ remains unassigned. On $^{18}O$ enrichment, each of the sharp bands gives rise to a sextet pattern, and Figure 6(*b*) shows the structure obtained on the $^{11}B$ component from a sample containing *ca.* 45% $^{18}O$. By varying the degree of enrichment, the various components could be related to specific $H_3{}^{11}B^{16}O_n{}^{18}O_{3-n}$ species, and the $^{10}B$ pattern although broader, could similarly be assigned.

Although the spectrum in Figure 6(*b*) can be related to the quartet patterns found in simpler molecules (*e.g.* $BCl_3$) where isotope substitution occurs in a degenerate mode,[23,24] the presence of *six* components here indicates that there is some interaction with at least one nearby mode, probably an HOB bend. This view is reinforced by the spectrum produced on deuterium enrichment, where both the bands at 1 478.0 and 1 426.2 $cm^{-1}$ again show a complex structure. Table 3 contains selected numerical data, and the assignments proposed here are again based on variations in relative intensity with enrichment.

A detailed vibrational analysis of this spectral region would require knowledge of the position of the *A*′ HOB bend, and also an accurate value of the HOB bond angle. Neither of these is currently available, and no attempt was therefore made to simulate these isotope patterns.

*Spectral region* 800—1 100 $cm^{-1}$. This spectral region contains one $H_3BO_3$ absorption at 1 009.9 $cm^{-1}$ which has been provisionally identified as the *E*′ HOB bend. It is at a significantly *lower* frequency than the corresponding assignment in the solid (Table 1) but similar in position to a band reported

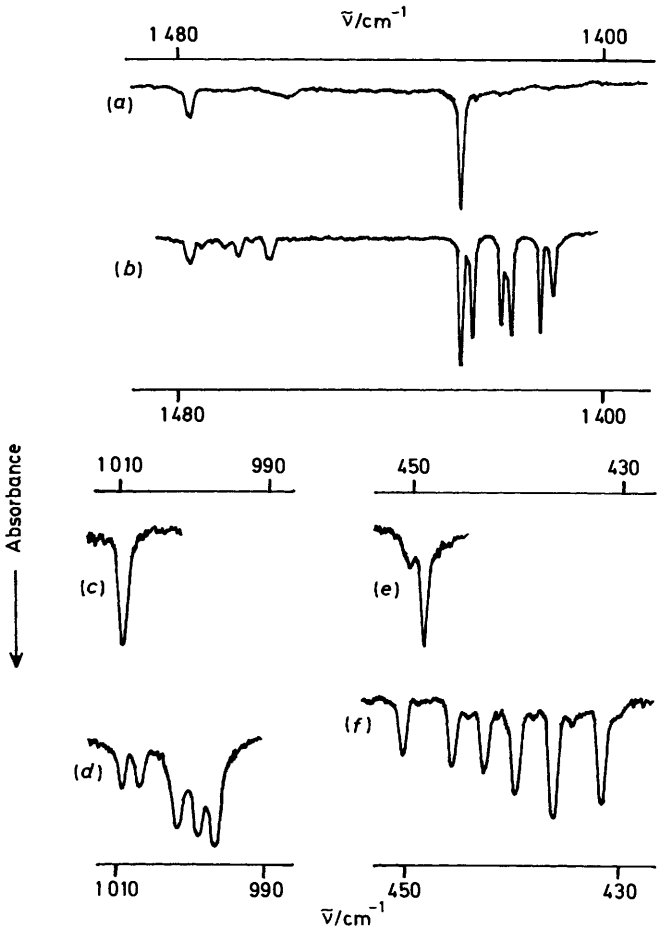


**Figure 6.** Isotope patterns associated with the $E'$ modes ν(BO), δ(HOB), and $\delta(BO_2)$. (*a*) ν(BO): normal isotopic composition; (*b*) ν(BO): 20% $^{10}B$, 45% $^{18}O$, 100% $^{1}H$; (*c*) δ(HOB): normal isotopic composition; (*d*) δ(HOB): 90% $^{10}B$, 60% $^{18}O$, 100% $^{1}H$; (*e*) $\delta(BO_2)$: normal isotopic composition; and (*f*) $\delta(BO_2)$: 90% $^{10}B$, 60% $^{18}O$, 100% $^{1}H$

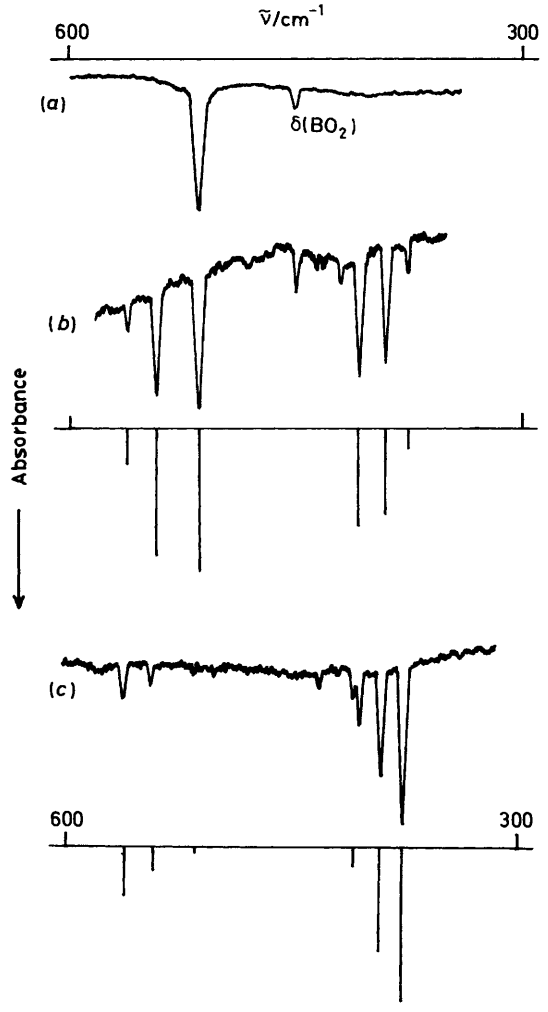


**Figure 7.** Isotope patterns associated with the torsion modes. (*a*) Spectrum obtained from normal boric acid, (*b*) observed and calculated spectra assuming 40% $^{2}D$ enrichment, and (*c*) observed and calculated spectra assuming 80% $^{2}D$ enrichment

in Margrave's vapour-phase study.[6] On deuteriation, a corresponding feature is observed at *ca.* 825 $cm^{-1}$ which we assign as the $E'$ DOB bend in $D_3BO_3$, and this large frequency shift is consistent with hydrogen atom motion. Partial enrichment with either deuterium or $^{18}O$ produced complex patterns, as anticipated for a degenerate mode, and although some of the components could be assigned (Table 3) by varying the isotopic composition, no attempt was made to simulate the spectra, primarily for the same reasons as discussed above. Representative spectra are included in Figure 6.

This spectral region is also important as regards possible weaker features. Raman studies have shown that both solid[1] and vapour-phase[25] boric acid exhibit an intense, polarised band at *ca.* 880 $cm^{-1}$, which according to the most recent assignment,[26] is identified as the symmetric $BO_3$ stretch. If this mode were to be found in our matrix i.r. studies, it would indicate a deviation from planarity for the $BO_3$ unit, and we therefore examined this spectral region under higher sensitivity in an attempt to locate this fundamental. However, even under conditions where the antisymmetric $BO_3$ stretch was effectively 100% absorbing, our matrix spectra of $H_3BO_3$ showed no evidence of the symmetric stretch.

*Spectral region* 300—600 $cm^{-1}$. The preliminary experiments identified two $H_3BO_3$ absorptions in this region, a relatively intense band at 513.8 $cm^{-1}$, and a weaker feature at 448.9 $cm^{-1}$. Higher resolution studies on these bands showed that whereas $^{10}B/^{11}B$, $^{16}O/^{18}O$, and $^{1}H/^{2}D$ isotope shifts could all be resolved for the band at 448.9 $cm^{-1}$ from suitably enriched samples, only deuterium enrichment produced a significant frequency shift for the 513.8 $cm^{-1}$ feature. This latter absorption is therefore identified as the $A''$ HOBO torsion mode, and the band at 448.9 $cm^{-1}$ assigned as the $E'$ in-plane $BO_2$ bend.

Figure 6(*e*) and (*f*) show representative spectra of the $E'$ bend first from a sample of 'normal' boric acid, and secondly from a sample enriched with $^{10}B$ (90 atom%) and $^{18}O$ (60 atom%). This latter spectrum shows the sextet pattern consistent with a degenerate vibration, and the components were assigned to specific isotopomers by correlating their intensities with the degree of $^{18}O$ enrichment. This mode also shows a modest deuterium isotope shift, with the corresponding band in $D_3BO_3$ occurring at *ca.* 405 $cm^{-1}$.

The more intense band at 513.8 $cm^{-1}$ shows a much greater deuterium isotope effect. Figure 7(*a*) shows the parent band under medium resolution, whilst Figure 7(*b*) and (*c*) show the effect of *ca.* 40 atom% and *ca.* 80 atom% deuterium enrichment respectively. New features appear both to high and low frequency of the parent band, and these could be assigned to appropriate isotopic species from the degree of enrichment. In particular the corresponding $D_3BO_3$ mode is identified at 376.0 $cm^{-1}$. In contrast to these large frequency shifts, the effect of $^{10}B$

or $^{18}O$ enrichment was merely to broaden or displace the band at 513.8 $cm^{-1}$ by *ca.* 1 $cm^{-1}$.

One surprising feature of these H/D patterns is the occurrence of two absorptions at *higher* frequency than the $H_3BO_3$ parent band, and their origin is not immediately obvious. Indeed, since the band at 513.8 $cm^{-1}$ is supposedly non-degenerate, its attendant isotope pattern should contain, at the most, only four components. However, in addition to providing one $A''$ mode, torsional motion in ($C_{3h}$) $H_3BO_3$ also yields one $E''$ mode. When the symmetry falls to $C_s$ in the partially substituted species, one of the components of this $E''$ mode gains i.r. intensity by mixing with the mode derived from the $A''$. The other component, whilst technically i.r. active, has zero intensity. The two 'extra' higher-frequency bands can thus be regarded as arising from the $E''$ mode. An analysis of the torsional modes has not previously been carried out for $C_s$ symmetry, and the Appendix summarises the relevant equations. Confirmation that the band at 513.8 $cm^{-1}$ is correctly assigned as the $A''$ torsion is then based on the results of this analysis.

In order to simulate the frequencies and relative intensities of the bands observed in Figure 7, 'reasonable estimates' for the B–O and O–H bond lengths are required for the calculation of the *G*-matrix elements. As indicated in the Appendix, the HOB angle was treated as a variable, and if one sets the bond length $r_{B-O}$ = 1.36 Å and $d_{O-H}$ = 0.95 Å, with angle HOB = 131°, the experimental isotope pattern can then be fitted to better than 1 $cm^{-1}$. Table 2 compares the observed and calculated frequencies for these torsion modes assuming harmonic vibrations, and also includes an estimated value for the inactive $E''$ mode. Figure 7 also shows the results of two spectral simulations which illustrate that the intensity fit is also very satisfactory.

This particular model, however, makes no allowance for anharmonicity, and if one regards the bond lengths as fixed parameters, it may readily be shown that the inclusion of a small anharmonic correction requires the choice of a different HOB angle in order to retain the fit. This bond angle will also act as a 'sink' for any errors introduced by the neglect of coupling with the out-of-plane $BO_3$ mode, and no particular significance should therefore be attached to the value emerging from this analysis.

However, it is of some interest to compare this estimate of *ca.* 130° for the HOB angle both with the predictions of *ab initio* calculations on $H_3BO_3$, and with experimentally determined angles in related molecules. In particular, Gundersen[27] has carried out a series of calculations on $H_3BO_3$ and related hydroxy–boron species.[28] These calculations indicate that HOB angles are expected to lie in the range 110–115°, and for some of the species considered [*e.g.* $HB(OH)_2$ and $H_2BOH$] there is supporting experimental evidence.[29] In $B(OMe)_3$, however,[17] and in other methoxyboranes,[30] the corresponding COB angles are significantly wider, and lie in the range 120—125°. Despite such variations, however, there is general agreement that the central $BO_3$ unit in all these species is planar, and that this structure receives additional stability from π bonding.

*Alternative structures for* $H_3BO_3$. Our matrix i.r. spectra for monomeric $H_3BO_3$ have been satisfactorily assigned on the assumption of $C_{3h}$ symmetry, but it is worth considering briefly whether an alternative shape might also be consistent with the observed spectra. The evidence for the presence of a $C_3$ axis is reasonably compelling, not only because of the $^{16}O/^{18}O$ isotope pattern associated with the $A''$ $BO_3$ mode, but because of the clear demonstration of degenerate modes. Coplanarity of the OH groups is indicated by the observation of only one OH stretch, and the central $BO_3$ group similarly appears to be planar, since there was no evidence for the symmetric $BO_3$ stretch in the parent $H_3BO_3$. The results thus provide no reason to suspect a symmetry lower than $C_{3h}$.

However, the observed spectra may in principle be assigned assuming a $D_{3h}$ model with linear BOH groups. For this geometry, $\Gamma_{vib.} = 2A_1' + A_2' + 2A_2'' + 4E' + 4E''$, with the i.r. active modes being $2A_2'' + 4E'$. As in the case of $C_{3h}$ symmetry, six i.r. bands are expected, and for five of these ($A_2'' + 4E'$) it turns out that the qualitative descriptions of the various modes (*e.g.* '*E*′B–O stretch') are the same for both point groups. The only difference lies in the description of the i.r. active out-of-plane hydrogen motion. In $D_{3h}$ symmetry this would be regarded as a BOH bend ($A_2''$) whilst in $C_{3h}$ it is the $A''$ torsion. Both types of vibration would be expected to occur at low frequency, and would show a large deuterium isotope effect. However, although the basic spectrum of $H_3BO_3$ could be assigned qualitatively assuming either symmetry, the magnitude of the deuterium isotope effect on this low-frequency out-of-plane mode can be used to distinguish the two symmetries.

As demonstrated above, the frequency shift from 513.8 $cm^{-1}$ ($H_3BO_3$) to 376.0 $cm^{-1}$ ($D_3BO_3$) can be reproduced exactly by choosing reasonable values for the geometrical parameters in $H_3BO_3$, and in the 'decoupled' approximation, this frequency shift is independent of force constant. The vibrational analysis for $D_{3h}$ $X(YZ)_3$ has been reported by Cyvin and co-workers,[31] and assuming a similar decoupling, the isotope shift from $H_3BO_3$ to $D_3BO_3$ for the $A_2''$ HOB bend is similarly independent of force constant. The corresponding *G* matrix term still includes the B–O and O–H bond lengths, but there is now no flexibility regarding the choice of HOB angle. Substitution of the same bond lengths ($r_{B-O}$ = 1.36 Å, $d_{O-H}$ = 0.95 Å) into the appropriate expression leads to a predicted $H_3BO_3$ to $D_3BO_3$ frequency shift of 513.8 to *ca.* 406 $cm^{-1}$. This is significantly less than the observed shift (513.8 to 376.0 $cm^{-1}$), and would require an appreciable anharmonic correction in order to fit the experimental data. In view of this, we regard the $D_{3h}$ model as less realistic, even on purely spectroscopic grounds.

## Conclusions

Mass spectrometric studies demonstrate that monomeric $H_3BO_3$ is a stable molecular species, and indicate that it is a major component in the vaporisation of orthoboric acid at *ca.* 40 °C. Subsequent matrix isolation studies show that the i.r. spectrum of $H_3BO_3$ has some features in common with the solid, but that all modes involving substantial hydrogen motion are significantly shifted in frequency. Extensive isotope enrichment experiments indicate that $H_3BO_3$ almost certainly has $C_{3h}$ symmetry, and although it was not possible to carry out a full vibrational analysis, estimates for some of the inactive fundamentals were obtained.

## Appendix

*Out-of-plane* $BO_3$ *Mode.*—If one assumes that this mode is decoupled from any torsion modes of the same symmetry, then it may be shown that the appropriate secular equation for all combinations of boron and oxygen isotopes is given by[32] equation (A1), where $M_B$, $M_{O_1}$, $M_{O_2}$, and $M_{O_3}$ are the masses of

$$\lambda = 4\pi^2\nu^2 = K\left(\frac{9}{M_B} + \frac{1}{M_{O_1}} + \frac{1}{M_{O_2}} + \frac{1}{M_{O_3}}\right) \quad \text{(A1)}$$

boron and oxygen atoms, and $K$ is a constant. The correct assignment of one isotopic component is sufficient to establish $K$, and thus to predict the frequencies of all other isotopic species. The relative intensities of the various components are then effectively determined by the appropriate statistical weightings.

OH *Stretching Modes.*—Within the framework of the high-frequency separation approximation, it may be shown that a set

of $G$-matrix elements suitable for all isotopic combinations of OH stretching motion is as given below, with all off-diagonal

$$G_{11} = \frac{1}{M_{H_1}} + \frac{1}{M_{O_1}};\ G_{22} = \frac{1}{M_{H_2}} + \frac{1}{M_{O_2}};\ G_{33} = \frac{1}{M_{H_3}} + \frac{1}{M_{O_3}}$$

terms set equal to zero; $M_{H_1}$, $M_{O_1}$, *etc.* are the appropriate masses of the hydrogen and oxygen atoms.

The $F$ matrix contains only two independent parameters: a principal stretching constant $F_d = F_{11} = F_{22} = F_{33}$, and a single interaction constant $F_{dd}$ which is equated with all the off-diagonal terms. The calculation of the isotope frequency and intensity patterns is then identical to that described previously.[20,21]

*Torsion Modes.*—The torsional modes in the $C_{3h}$ parent species (*e.g.* $H_3BO_3$) transform as $A'' + E''$, and the corresponding $G$-matrix elements have been given by Cyvin *et al.*[18] However, these relationships cannot be applied to lower symmetry species such as $H_2DB^{16}O_3$ or $H_3B^{16}O_2{}^{18}O$, and we have therefore derived expressions appropriate for the more general $C_s$ symmetry species $X(YZ)_3$ in which all combinations of isotopic masses are allowed. Using the geometrical parameters defined in Figure 3(*a*), one may envisage three torsional 'symmetry' co-ordinates $T_1 = (rd)^{\frac{1}{2}}\tau_1$, $T_2 = (rd)^{\frac{1}{2}}\tau_2$, and $T_3 = (rd)^{\frac{1}{2}}\tau_3$. Application of standard procedures[33] then leads to the $G$-matrix elements given below, where $M_X$, $M_{Y_1}$, $M_{Z_1}$, *etc.* are

$$G_{11} = \frac{A}{M_{Z_1}} + \frac{B}{M_{Y_1}} + \frac{C}{M_X} + \frac{D}{M_{Y_3}}$$

$$G_{22} = \frac{A}{M_{Z_2}} + \frac{B}{M_{Y_2}} + \frac{C}{M_X} + \frac{D}{M_{Y_1}}$$

$$G_{33} = \frac{A}{M_{Z_3}} + \frac{B}{M_{Y_3}} + \frac{C}{M_X} + \frac{D}{M_{Y_2}}$$

$$G_{12} = G_{21} = \frac{C}{M_X} + \frac{E}{M_{Y_1}}$$

$$G_{13} = G_{31} = \frac{C}{M_X} + \frac{E}{M_{Y_3}}$$

$$G_{23} = G_{32} = \frac{C}{M_X} + \frac{E}{M_{Y_2}}$$

the masses of atoms X, Y, Z, *etc.*, and the constants $A$—$E$ have the following values: $A = (r/d)\mathrm{cosec}^2\beta$, $B = (r/d)\mathrm{cosec}^2\beta - 2\mathrm{cosec}\beta(\cot\beta + 1/\sqrt{3}) + (d/r)(\cot\beta + 1/\sqrt{3})^2$, $C = (d/r)(\cot\beta + \sqrt{3})^2$, $D = \frac{4}{3}(d/r)$, and $E = (2/\sqrt{3})[(\cot\beta + 1/\sqrt{3})(d/r) - \mathrm{cosec}\beta]$. The corresponding $F$ matrix is defined in terms of two parameters $F_\tau$ and $F_{\tau\tau}$, with $F_{11} = F_{22} = F_{33} = F_\tau$, and all the off-diagonal terms set equal to $F_{\tau\tau}$. As indicated above, there are good reasons for treating the out-of-plane torsional modes in boric acid as being effectively decoupled from out-of-plane $BO_3$ motion.

The solution[33] of the determinantal equation $GF - I\lambda = 0$ was carried out for each isotopic species, but inspection of the $G$ matrix shows that this requires suitable estimates for the bond lengths $r_{B-O}$ and $d_{O-H}$ and for the HOB angle $\beta$. An estimate of $r = 1.36$ Å is available from structural studies on the solid,[9,12,13] and we arbitrarily chose a value for the O–H bond length of 0.95 Å. Variations in these parameters by up to $\pm 10\%$ did not significantly affect the ultimate calculation of isotope patterns. The angle parameter $\beta$, together with the two force constants $F_\tau$ and $F_{\tau\tau}$ were then treated as variables in an attempt to reproduce all six observed torsion frequencies.

Relative band intensities were calculated by assuming that the changes $\partial\mu/\partial\tau$ produced by torsional motion could be treated in a similar way to bond dipole derivatives. This leads to intensity relationships identical to those used in the more familiar bond dipole model.[33] The resulting intrinsic intensities were then multiplied by the appropriate statistical weightings in order to simulate a particular experimental spectrum.

## Acknowledgements

We gratefully acknowledge the financial support of the S.E.R.C. and the UK AEA (Winfrith) for the provision of a CASE studentship, and also wish to thank Dr. T. R. Gilson for Raman studies.

## References

1 See, *e.g.* R. W. Sprague, in 'A Comprehensive Treatise on Inorganic and Theoretical Chemistry,' ed. J. W. Mellor, Longmans, London, 1980, vol. 5, suppl. 1, part A.
2 See, *e.g.* P. W. Atkins, M. S. Child, and C. S. G. Phillips, 'Tables for Group Theory,' Oxford University Press, 1970.
3 C. W. F. T. Pistorius, *J. Chem. Phys.*, 1959, **31**, 1454.
4 JANAF, 'Thermochemical Tables,' 2nd edn., NSRDS-NBS 37, *Nat. Bur. Stand. (U.S.)*, 1971.
5 D. J. Meschi, W. A. Chupka, and J. Berkowitz, *J. Chem. Phys.*, 1960, **33**, 530.
6 F. T. Greene, G. E. Leroi, S. P. Randall, J. R. Soulen, L. H. Spinar, and J. L. Margrave, Proceedings of the Propellant Thermodynamics and Handling Conference, 1959, July 20—21, Ohio State University, Special Report, 1960, vol. 12, p. 23.
7 M. v. Stackelberg, F. Quatram, and J. Dressel, *Z. Elektrochem.*, 1937, **43**, 14.
8 H. Tazaki, *J. Sci. Hiroshima*, 1940, **10A**, 37.
9 W. H. Zachariasen, *Acta Crystallogr.*, 1954, **7**, 305.
10 E. G. Hope, P. J. Jones, W. Levason, J. S. Ogden, M. Tajik, and J. W. Turff, *J. Chem. Soc., Dalton Trans.*, 1985, 1443.
11 L. A. Kristiansen, R. W. Mooney, S. J. Cyvin, and J. Brunvoll, *Acta Chem. Scand.*, 1965, **19**, 1749.
12 J. M. Cowley, *Acta Crystallogr.*, 1953, **6**, 522.
13 B. M. Craven and T. M. Sabine, *Acta Crystallogr.*, 1966, **20**, 214.
14 D. E. Bethell and N. Sheppard, *Trans. Faraday Soc.*, 1955, **51**, 9.
15 R. R. Servoss and H. M. Clark, *J. Chem. Phys.*, 1957, **26**, 1175.
16 J. L. Margrave and S. P. Randall, personal communication quoted by R. Ottinger, S. J. Cyvin, R. W. Mooney, L. A. Kristiansen, and J. Brunvoll, *Acta Chem. Scand.*, 1966, **20**, 1389.
17 G. Gundersen, *J. Mol. Struct.*, 1976, **33**, 79.
18 S. J. Cyvin, R. W. Mooney, J. Brunvoll, and L. A. Kristiansen, *Acta Chem. Scand.*, 1965, **19**, 1031.
19 A. J. Tursi and E. R. Nixon, *J. Chem. Phys.*, 1970, **52**, 1521.
20 J. H. Darling and J. S. Ogden, *J. Chem. Soc., Dalton Trans.*, 1972, 2496.
21 H. Huber, E. P. Kundig, M. Moskovits, and G. A. Ozin, *J. Am. Chem. Soc.*, 1973, **95**, 332.
22 See, *e.g.* G. Herzberg, 'Molecular Spectra and Molecular Structure,' vol. I: Spectra of Diatomic Molecules,' Van Nostrand, Princeton, New Jersey, 1950.
23 I. R. Beattie, H. E. Blayden, S. M. Hall, S. N. Jenny, and J. S. Ogden, *J. Chem. Soc., Dalton Trans.*, 1976, 666.
24 J. S. Ogden, *Ber. Bunsenges. Phys. Chem.*, 1978, **83**, 76.
25 T. R. Gilson, unpublished work.
26 R. Janda and G. Heller, *Spectrochim. Acta, Part A*, 1980, **36**, 997.
27 G. Gundersen, *Acta Chem. Scand., Ser. A*, 1981, **35**, 729.
28 T. Fjeldberg, G. Gundersen, T. Jonvik, H. M. Seip, and S. Saebo, *Acta Chem. Scand., Ser. A*, 1980, **34**, 547.
29 Y. Kawashima, H. Takeo, and C. Matsumura, *J. Chem. Phys.*, 1981, **74**, 5430.
30 G. Gundersen, T. Jonvik, and R. Seip, *Acta Chem. Scand., Ser. A*, 1981, **35**, 325.
31 R. W. Mooney, S. J. Cyvin, and J. Brunvoll, *Acta Chem. Scand.*, 1965, **19**, 983.
32 S. N. Jenny and J. S. Ogden, *J. Chem. Soc., Dalton Trans.*, 1979, 1465.
33 See, *e.g.* E. B. Wilson, jun., J. C. Decius, and P. C. Cross, 'Molecular Vibrations,' McGraw-Hill, New York, 1955.

*Received* 30*th July* 1987; *Paper* 7/1389